

Journal of Organometallic Chemistry, 368 (1989) 339–350
Elsevier Sequoia S.A., Lausanne – Printed in The Netherlands
JOM 09817

Substituted cyclopentadienyl complexes

VII *. An NMR and X-ray crystallographic study of $[(\eta^5\text{-C}_5\text{H}_4\text{R})\text{Fe}(\text{CO})(\text{PPh}_3)\text{I}]$ ($\text{R} = \text{CHPh}_2, \text{I}, \text{CH}(\text{CH}_3)_2$)

Johan du Toit, Demetrius C. Levendis, Jan C.A. Boeyens, Mohamed S. Loonat,
Laurence Carlton, Wolfgang Pickl and Neil J. Coville *

Department of Chemistry, University of the Witwatersrand, Johannesburg (R.S.A.)

(Received August 23rd, 1988)

Abstract

The complexes $[(\eta^5\text{-C}_5\text{H}_4\text{R})\text{Fe}(\text{CO})(\text{PPh}_3)\text{I}]$ ($\text{R} = \text{I}$ (**1**), $\text{CH}(\text{CH}_3)_2$ (**2**), CHPh_2 (**3**)) have been synthesised. The NOE spectra recorded on the new complexes reveal a preferential conformation of the ring substituent on **3**, with the H atom of the benzhydryl group pointing towards the PPh_3 ligand. A similar effect is not observed in the spectrum of **2**. The phenomenon is related to the steric effect associated with the relative sizes of the ring substituents.

The crystal structures of **1** and **3** have been determined. The results for **3** suggest that the dominant conformer observed in solution corresponds to the solid state structure.

Introduction

In recent years it has become apparent that the rotational behaviour of aromatic hydrocarbon rings in complexes of the type $(\text{ring})\text{MA}_x$ can be detected and is influenced by both the A_x ligand set [1] and the ring substituent [2]. From these considerations it would be expected that the conformational preferences of the ring substituents could also be detected by the correct choice of the metal, ligands and ring substituents. Indeed, electronic barriers to the rotation of acyl ring substituents in substituted ferrocene [3] and ruthenocene [4] complexes have been measured. To our knowledge, however, the detection of steric influences on ring substituent conformations in the above types of complexes has not been reported.

* For part VI see ref. 2.

We report here our NMR data on $[(\eta^5\text{-C}_5\text{H}_4\text{R})\text{Fe}(\text{CO})(\text{PPh}_3)\text{I}]$ ($\text{R} = \text{I}$ (1), Pr^i (2), CHPh_2 (3)), which confirm that steric factors influence the conformation of the CHPh_2 substituent in $[(\eta^5\text{-C}_5\text{H}_4\text{CHPh}_2)\text{Fe}(\text{CO})(\text{PPh}_3)\text{I}]$. Also reported are the X-ray crystal structure determinations of $[(\eta^5\text{-C}_5\text{H}_4\text{R})\text{Fe}(\text{CO})(\text{PPh}_3)\text{I}]$ ($\text{R} = \text{I}$, CHPh_2), which have provided solid state data on minimum energy conformations of the various ligands.

Experimental

$[\text{Fe}(\text{CO})_5]$ was purchased from Strem Chemicals. The 6,6-dimethylfulvene [5] and 6,6-diphenylfulvene [6] were prepared by literature procedures and the isopropyl- [7,8] and benzydrylcyclopentadienes [7] were prepared from the corresponding fulvenes by reduction with LiAlH_4 .

Diazocyclopentadiene was prepared by either the method described by Regitz and Liedhegener [9] by diazotransfer from tosylazide to cyclopentadiene in acetonitrile/diethylamine, or by the method described by Weil and Cais [10–12] but using diethylamine (rather than ethanolamine, which gave low yields) as base. The required material was purified by chromatography on silica gel with benzene as eluent [12]. The concentration of the resulting benzene solution was determined by ^1H NMR spectroscopy using an internal standard, and this solution was used directly in the preparation of $[(\eta^5\text{-C}_5\text{H}_4\text{I})\text{Fe}(\text{CO})_2\text{I}]$ [12]. IR spectra were recorded on a Perkin–Elmer 580B spectrometer and ^1H NMR spectra on a Bruker AC 200 spectrometer. NOE spectra were recorded as described previously [1].

Preparation of $[(\eta^5\text{-C}_5\text{H}_4\text{Pr}^i)\text{Fe}(\text{CO})_2]_2$

$[\text{Fe}_2(\text{CO})_9]$ (12 g; 32 mmol) and isopropylcyclopentadiene (3 g, 28 mmol) were added to dry benzene (80 ml) and the mixture was stirred under N_2 at room temperature; it became dark-red, on stirring. Product formation was monitored by TLC. After 24 h the black mixture was pumped to dryness to yield 7.3 g of a dark red liquid (59% crude yield). Recrystallization from CH_2Cl_2 and petroleum ether gave fine black needles of the required product with m.p. $63\text{--}64^\circ\text{C}$. IR (CH_2Cl_2) $\nu(\text{CO})$: 1979, 1949, 1763 cm^{-1} ; ^1H NMR (C_6D_6): C_5H_4 , 4.36t, 3.99t; $\text{CH}(\text{CH}_3)_3$, 2.74 s ($J(\text{H}\text{--}\text{H})$ 6.8; $\text{CH}(\text{CH}_3)_2$, 1.12d, $J(\text{H}\text{--}\text{H})$ 6.8.

Preparation of $[(\eta^5\text{-C}_5\text{H}_4\text{CHPh}_2)\text{Fe}(\text{CO})_2]_2$

$[\text{Fe}_2(\text{CO})_9]$ (2.5 g, 6.5 mmol) and benzydrylcyclopentadiene (1.4 g, 6 mmol) were added to dry benzene (30 ml) and the mixture was stirred under N_2 at room temperature. The solution became dark-red on stirring as the $[\text{Fe}_2(\text{CO})_9]$ dissolved. Product formation was monitored by TLC. After 24 h the black mixture was pumped to dryness to yield a black solid (987 mg, 70% yield). Recrystallization from petroleum ether and CH_2Cl_2 gave 900 mg of dark black plates of the required complex. ^1H NMR (C_6D_6): C_5H_4 , 4.05 s, CHPh_2 , 5.88(s).

Preparation of $[(\eta^5\text{-C}_5\text{H}_5\text{Pr}^i)\text{Fe}(\text{CO})_2\text{I}]$

$[(\eta^5\text{-C}_5\text{H}_4\text{Pr}^i)\text{Fe}(\text{CO})_2]_2$ (3.0 g, 6.9 mmol) was dissolved in CH_2Cl_2 (20 ml) and a solution of I_2 (2 g $\text{I}_2/100$ ml CH_2Cl_2) added dropwise to the stirred solution under N_2 . The reaction was monitored by IR spectroscopy and was considered to be complete when the IR ($\nu(\text{CO})$) absorption at ca. 1760 cm^{-1} had disappeared (2 h).

Table 1

¹H NMR data for 1, 2 and 3^a

Complex	Cyclopentadienyl ring ^b					Ring substituent ^b		PPh ₃ ^b	
	H2	H3	H4	H5	Δ(H2-H5)	H	Me or Ph ^c	<i>ortho</i>	<i>meta/para</i>
1	4.91	4.14	3.43	3.77	1.14	—	—	7.66m	6.97m
2	5.04	4.56	3.38	3.27	1.77	2.92(s)	1.19(d), 1.07(d)	7.75m	6.99m
3	3.81	2.38	4.33	5.14	1.33	6.13	7.7m, 7.0m	7.62d, 7.22d	7.0m

^a Recorded in C₆D₆ relative to TMS. ^b (ppm); m = multiplet, s = septet, d = doublet. ^c *ortho*-protons listed.

The excess of I₂ was removed by shaking the mixture with aqueous Na₂S₂O₃, and the organic layer was dried (MgSO₄) and concentrated to give a dark black oil. Column chromatography (column packed with silica/hexane slurry; elution with benzene) gave a black oil, judged to be pure from its IR and NMR spectra (49% yield). IR (CH₂Cl₂) ν(CO): 2044, 1989 cm⁻¹; ¹H NMR (C₆D₆) C₅H₄, 4.02m, 4.04m; CH(CH₃)₂, 2.27q *J*(H-H) 6.8; CH(CH₃)₂, 0.81d *J*(H-H) 6.8.

Preparation of [(η⁵-C₅H₄Pr¹)Fe(CO)(PPh₃)I]

[(η⁵-C₅H₄Pr¹)Fe(CO)₂I] (346 mg, 1 mmol) and PPh₃ (262 mg, 1 mmol) were dissolved in benzene (10 ml). The solution was brought to reflux and [(η⁵-C₅H₅)Fe(CO)₂]₂ (10 mg) added as catalyst. The reaction was monitored by IR spectroscopy and was complete within 2.5 h. The solution was pumped to dryness, crude product redissolved in benzene, and the black solution passed through an alumina column (eluent, benzene). The first small yellow band was not characterized. The second green band was collected, the solution pumped to dryness, and the green solid (m.p. 129–130 °C, 67% yield) characterized by IR (ν(CO), CH₂Cl₂ 1940 cm⁻¹) and NMR spectroscopy (Table 1).

Preparation of [(η⁵-C₅H₄CHPh₂)Fe(CO)(PPh₃)I]

[(η⁵-C₅H₄CHPh₂)Fe(CO)₂I] (175 mg, 0.37 mmol) and PPh₃ (97 mg, 0.37 mmol) were dissolved in benzene (5 ml). The solution was brought to reflux and [(η⁵-C₅H₅)Fe(CO)₂]₂ (5 mg) added as catalyst. The reaction, monitored by IR spectroscopy, was complete in less than 3 h. The crude material was passed through a silica column (eluent, benzene) and revealed a small and a large green band. The slower moving larger green fraction was collected and the solvent removed to yield a green solid (m.p. 170–171 °C 55% yield), characterized by IR (ν(CO), CH₂Cl₂: 1944 cm⁻¹) and NMR spectroscopy (Table 1).

Preparation of [(η⁵-C₅H₄I)Fe(CO)(PPh₃)I]

[(η⁵-C₅H₄I)Fe(CO)₂I] (223 mg, 0.5 mmol) and PPh₃ (131 mg, 0.5 mmol) were dissolved in benzene (7 ml). The solution was brought to reflux and catalyst [(η⁵-C₅H₄)Fe(CO)₂]₂ (10 mg) added. The reaction was monitored by IR spectroscopy and was considered complete in 1 h. Passage of the crude material through a silica column with benzene as eluent gave a green fraction from which the required solid (dec. 156 °C), characterized by IR (ν(CO) CH₂Cl₂ 1955 cm⁻¹ and NMR spectroscopy (Table 1), was obtained (69% yield). The reaction was also carried out by allowing a benzene solution of the reactants to stand in sunlight (0.5 h).

Table 2

Crystal data, acquisition and refinement details for **1** and **3**

Complex	1	3
Formula	C ₂₄ H ₁₉ FeI ₂ OP	C ₃₇ H ₃₀ FeIOP
<i>M_r</i>	664.03	704.36
Colour, shape	Black needles	Black needles
Space group	<i>Pna</i> 2 ₁	<i>P</i> 2 ₁ / <i>c</i>
<i>a</i> /Å	16.231(3)	12.852(2)
<i>b</i> /Å	18.342(2)	14.585(5)
<i>c</i> /Å	7.748(2)	17.481(2)
β /°	90.00(2)	107.96(1)
<i>V</i> /Å ³	2306.65	3116.89
<i>Z</i>	4	4
<i>F</i> (000)	1272	1416
<i>D_c</i> /g·cm ⁻³	1.912	1.501
<i>K_α</i> used/Å	Cu: 1.542	Mo: 0.7107
μ /cm ⁻¹	41.3	10.3
Scan mode	$\omega/2\theta$	$\omega/2\theta$
Scan range/°	3 ≤ θ ≤ 65	2 ≤ θ ≤ 27
Scan speed/°·min ⁻¹	5.5	5.5
<i>h</i>	0 → 18	-16 → 16
<i>k</i>	0 → 21	0 → 18
<i>l</i>	0 → 9	0 → 22
Measured intensities	2278	7291
Unique reflections	2085	6093
Internal consistency	0.000	0.019
Omitted reflections	75	1297
Cut-of criterion	<i>F</i> > 2σ(<i>F</i>)	<i>F</i> > 3σ(<i>F</i>)
No. of parameters	137	371
Maximum $\Delta p/\sigma$	0.14	0.28
Res. density/e Å ⁻³	1.90	0.350
<i>R</i>	0.058	0.033
<i>R_w</i> ^a	0.056	0.028
Weighting coeff. $w = K/\sigma^2 F$	1.416	1.538

$$^a R_w = \frac{\sum \sqrt{w} [|F_o| - |F_c|]}{\sum \sqrt{w} [|F_o|]}$$

Crystal structure determination

Single crystals of **1** and **3**, grown from toluene/hexane were mounted on glass fibres. Preliminary investigation of [(η⁵-C₅H₄I)Fe(CO)(PPh₃)I] (**1**) and [(η⁵-C₅H₄CHPh₂)Fe(CO)(PPh₃)I] (**3**) was carried out by standard Weissenberg and precession photography. Crystallographic analyses were based on X-ray diffraction data collected with an automatic Enraf-Nonius CAD4 four-circle single-crystal diffractometer, using graphite monochromated Cu-*K_α* and Mo-*K_α* radiation, respectively. Refined cell constants were measured and refined from 25 accurately measured reflections in the range 25° ≤ θ ≤ 35° (for complex **1**) and 16° ≤ θ ≤ 19° (for complex **3**). Standard reflections were measured every hour of exposure time. Each data set was corrected for crystal decay and Lorentz-polarisation effects. An empirical absorption correction [13] was applied to each data set. The crystal data and crystallographic details are shown in Table 2.

The structures of **1** and **3** were solved by Patterson methods, and subsequent Fourier synthesis revealed the remaining non-hydrogen atoms. Refinement was

Table 3

Fractional coordinates ($\times 10^4$) and equivalent isotropic temperature factors ($\text{\AA}^2 \times 10^3$) for non-hydrogen atoms

Complex 1				
	<i>x</i>	<i>y</i>	<i>z</i>	U_{eq}
Fe	3456(1)	2502(1)	-270(5)	33(1)
I(1)	1994(1)	1906(1)	0	37
I(2)	4400(1)	725(1)	1153(3)	70
P	2992(3)	3502(2)	-1644(7)	27(1)
O	3741(7)	1790(6)	-3556(18)	38(3)* ^a
C(1)	4234(11)	1825(9)	1207(30)	34(4)*
C(2)	3684(13)	2164(12)	2244(29)	42(6)*
C(3)	3785(13)	2978(11)	2088(30)	49(6)*
C(4)	4410(11)	3068(9)	887(27)	43(5)*
C(5)	4669(11)	2365(9)	440(26)	42(5)*
C(6)	3609(12)	2058(10)	-2378(26)	31(5)*
C(7)	2069(10)	3405(9)	-2991(23)	26(4)*
C(8)	2083(11)	2933(9)	-4368(26)	40(5)*
C(9)	1385(11)	2788(10)	-5361(30)	45(5)*
C(10)	679(11)	3160(10)	-4291(34)	47(5)*
C(11)	652(12)	3682(9)	-3750(33)	44(5)*
C(12)	1331(11)	3804(10)	-2663(28)	40(5)*
C(13)	2696(10)	4232(8)	-201(27)	30(4)*
C(14)	2161(10)	4062(9)	1165(27)	34(4)*
C(15)	1877(11)	4562(10)	2351(27)	38(5)*
C(16)	2128(11)	5270(10)	2200(29)	44(5)*
C(17)	2652(12)	5459(10)	842(29)	46(5)*
C(18)	2943(10)	4948(9)	-344(24)	34(4)*
C(19)	3696(10)	3936(9)	-3206(23)	28(4)*
C(20)	4504(10)	3676(9)	-3369(25)	34(4)*
C(21)	5052(12)	3976(10)	-5433(27)	49(5)*
C(22)	4773(13)	4551(10)	-5576(29)	50(6)*
C(23)	3972(12)	4823(11)	-5439(29)	48(5)*
C(24)	3431(11)	4501(10)	-4263(27)	41(5)*

^a* isotropic temperature factor.

carried out using full-matrix least-squares calculations in which the hydrogen atoms were included at calculated positions. For complex 1 only the four heaviest atoms were assigned anisotropic temperature factors, while for 3 all the non-hydrogen atoms were refined anisotropically. The *R* values converged to 0.058 and 0.033 for complexes 1 and 3, respectively. All calculations were performed on a Cyber-750 computer (complex 1) and on a IBM PC-XT computer fitted with a Definicon board (complex 3) using the SHELX-86 [14] system of programs. Final positional parameters for 1 and 3 are given in Tables 3 and 4. Lists of anisotropic thermal parameters, hydrogen coordinates, and observed and calculated structure factors are available from the authors.

Results and discussion

The syntheses of the $[(\eta^5\text{-C}_5\text{H}_5)\text{Fe}(\text{CO}_2)]_2$, $[(\eta^5\text{-C}_5\text{H}_4\text{R})\text{Fe}(\text{CO})_2\text{I}]$ and $[(\eta^5\text{-C}_5\text{H}_4\text{R})\text{Fe}(\text{CO})(\text{PPh}_3)\text{I}]$ (R = I, ¹Pr, CHPh₂) complexes were carried out by stan-

Table 4

Fractional coordinates ($\times 10^4$) and equivalent isotropic temperature factors ($\text{\AA}^2 \times 10^3$) for non-hydrogen atoms of complex 3

	x	y	z	U_{eq}
I(1)	2711	858	1698	50
Fe	2744	-667	2500	41
P	1238(1)	-323(1)	2821(1)	41
O	4122(2)	-21(2)	4007(2)	77(1)
C(1)	3739(3)	-1360(2)	1925(2)	46(1)
C(2)	3818(3)	-1780(3)	2668(2)	53(1)
C(3)	2773(3)	-2086(3)	2661(3)	57(1)
C(4)	2033(3)	-1882(3)	1900(3)	55(1)
C(5)	2615(3)	-1431(2)	1447(2)	48(1)
C(6)	4649(3)	-976(3)	1643(2)	48(1)
C(7)	5669(3)	-771(3)	2349(3)	54(1)
C(8)	5857(4)	116(3)	2645(3)	75(1)
C(9)	6753(4)	294(4)	3308(4)	97(2)
C(10)	7453(4)	-385(4)	3673(3)	92(2)
C(11)	7285(4)	-1264(4)	3382(3)	81(1)
C(12)	6394(3)	-1452(3)	2713(3)	67(1)
C(13)	4881(3)	-1583(3)	1007(2)	51(1)
C(14)	4680(4)	-2504(3)	953(3)	72(1)
C(15)	4919(4)	-3029(4)	372(3)	92(2)
C(16)	5365(4)	-2621(5)	-157(3)	106(2)
C(17)	5566(4)	-1717(4)	-118(3)	105(2)
C(18)	5328(3)	-1185(3)	470(2)	78(1)
C(19)	3586(3)	-226(2)	3435(2)	56(1)
C(21)	-43(3)	-177(2)	1998(2)	46(1)
C(22)	-59(3)	-344(2)	1215(2)	48(1)
C(23)	-1027(3)	-276(3)	587(2)	59(1)
C(24)	-1974(3)	-38(3)	729(3)	74(1)
C(25)	-1969(3)	137(3)	1502(3)	83(1)
C(26)	-1005(3)	72(3)	2132(3)	69(1)
C(31)	1231(3)	656(2)	3480(2)	45(1)
C(32)	1834(3)	1438(2)	3470(2)	56(1)
C(33)	1777(3)	2186(3)	3949(2)	69(1)
C(34)	1127(4)	2152(3)	4448(3)	76(1)
C(35)	536(4)	1371(3)	4462(3)	77(1)
C(36)	580(3)	624(3)	3996(2)	61(1)
C(41)	954(3)	-1277(2)	3403(2)	44(1)
C(42)	1680(3)	-1423(3)	4172(2)	56(1)
C(43)	1574(3)	-2177(3)	4614(3)	67(1)
C(44)	735(4)	-2782(3)	4306(3)	69(1)
C(45)	21(3)	-2653(3)	3551(3)	68(1)
C(46)	127(3)	-1905(3)	3096(2)	56(1)

standard procedures, and the complexes were routinely characterised as described in the Experimental section. Complexes 1, 2 and 3 are all relatively air stable green compounds.

NOE spectroscopy was used to relate the ^1H NMR signals to the cyclopentadienyl ring protons as described previously [1], and Fig. 1 indicates the numbering scheme employed for the protons and associated resonances under investigation. The conformational preference of the ring relative to the ligand set could readily be

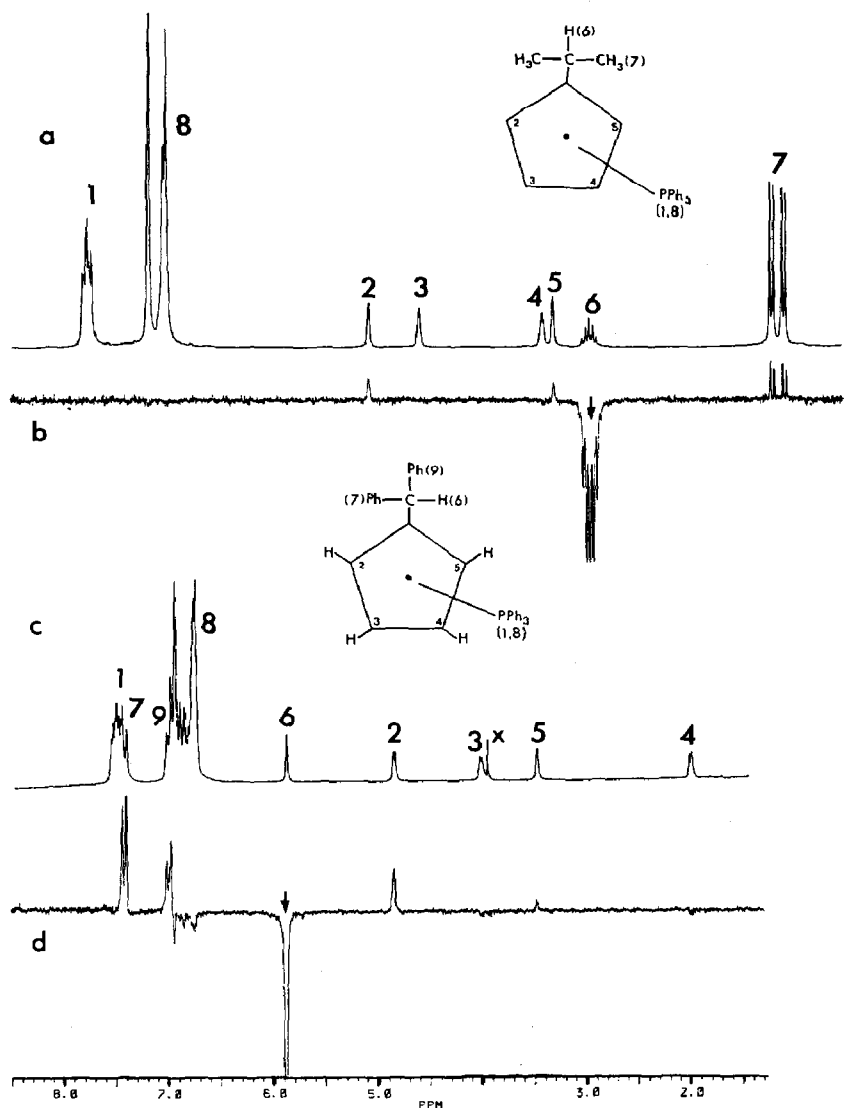


Fig. 1. (a) ^1H NMR spectrum of $[(\eta^5\text{-C}_5\text{H}_4^1\text{Pr})\text{Fe}(\text{CO})(\text{PPh}_3)\text{I}]$; (b) NOE spectrum of $[(\eta^5\text{-C}_5\text{H}_4^1\text{Pr})\text{Fe}(\text{CO})\text{PPh}_3]\text{I}$ showing irradiation of the ^1Pr hydrogen atom; (c) ^1H NMR spectrum of $[(\eta^5\text{-C}_5\text{H}_4\text{CHPh}_2)\text{Fe}(\text{CO})(\text{PPh}_3)\text{I}]$ ($\text{X} = \text{impurity}$); (d) NOE spectrum of $[(\eta^5\text{-C}_5\text{H}_4\text{CHPh}_2)\text{Fe}(\text{CO})(\text{PPh}_3)\text{I}]$ showing irradiation of the benzhydryl hydrogen atom.

detected in 1 to 3 by the NOE technique. Thus, irradiation of the *ortho*-phenyl protons of the PPh_3 ligand in 1 and 2 resulted in various increases in the intensity of the resonances associated with ring protons H2–H5. The variation in the increased intensity correlates with the time the *ortho* protons are close to the ring protons, and hence provides a means of establishing probable ligand conformations. For 1 there was almost equal growth of all four resonances associated with H2–H5, suggesting near equal occupancy of all possible conformations of the ring relative to the ligand set. The NOE spectrum of 2, however, indicates only a small increase for the resonance associated with H2 (30%) relative to the H3, H4 and H5 protons. This

is consistent with a dominant conformation in which the PPh_3 ligand protons are situated close to H3–H5 and far away from H2 i.e. with the PPh_3 ligand situated close to C4. This is also consistent with $J(\text{P-H})$ data; the P–H coupling involving H4 is much larger than that involving H2. Visual inspection also reveals that H3 and H4 are associated with broader resonances than the H2 and H5 protons (see Fig. 1a), a feature which arises from the larger PPh_3 coupling to H3 and H4.

Owing to the overlap of the resonance of the *ortho* ring protons of PPh_3 on 3 with some of the resonances of the *ortho* ring protons of the CHPh_2 ligand it was not possible to apply the same procedure to 3 in order to establish ring conformational data. Instead consecutive irradiation of protons H2–H5 revealed that only H3, H4, and H5 resulted in growth of the *ortho* phenyl proton resonances of PPh_3 (resonance 1 in Fig. 1c). NMR data are again consistent with location of the PPh_3 ligand preferentially close to C4.

The NOE study also provided information on the conformational preferences of the groups on the ring substituent relative to the cyclopentadienyl ring i.e. of the Ph, Me and H groups relative to the bond connecting the C_{ipso} ring carbon atom and the carbon atom of the substituent. Thus, irradiation of the ^1Pr methine hydrogen atom resulted in equal growth of H2 and H5 (3.5% growth for both resonances, Fig. 1b). The methyl groups associated with the ^1Pr substituent either have equal access to all conformations or a preferential conformation with the H atom pointing towards the Fe atom, i.e. between H2 and H5. Both situations would lead to equivalence of the intensities of the H2 and H5 resonances. The NOE data did, however, provide definitive evidence for a conformational preference of the CHPh_2 substituents relative to the cyclopentadienyl ring and the ligand set. Thus irradiation of the benzhydryl proton resulted in growth of two resonances at δ 7.5 that are due to the four *ortho* protons on the two substituent phenyl groups (Fig. 1d). The irradiation of the benzhydryl hydrogen atoms also resulted in the appearance of resonances associated with H5 and H2. Significantly these resonances had different intensities (H5 (6%) and H2 (1%)), corresponding to ca. 85/15 ratio. Further, irradiation of H2 resulted in the growth of only one of the *ortho* phenyl ring resonances of the CHPh_2 group. The data can readily be rationalised by assuming the dominance of the conformation shown in Fig. 2.

The differences in the conformations of the ring substituents in 1 and 3 is related to the steric size of the groups (Me versus Ph) attached to the ring substituent. Attempts are presently underway to further explore and delineate this phenomenon

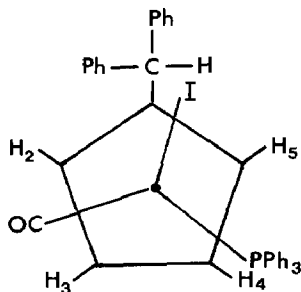


Fig. 2. Proposed structure for the $[(\eta^5\text{-C}_5\text{H}_4\text{CHPh}_2)\text{Fe}(\text{CO})(\text{PPh}_3)\text{I}]$ as determined from the ^1H NMR spectra.

Table 5

Selected bond lengths (Å) and angles (°) for **1**, **3** and **4**

	1	3	4
Fe–I	2.621(3)	2.624(1)	2.618(1)
Fe–P	2.250(5)	2.231(1)	2.234(1)
Fe–C _{carbonyl}	1.84(2)	1.781(4)	1.769(6)
C _{carbonyl} –O	1.06(2)	1.067(4)	1.096(6)
(Fe–C _{ring}) _{ave}	2.08	2.11	2.11
Fe–Cen ^a	1.708	1.721	1.731
(P–C) _{ave}	1.830	1.832	1.830
(Fe–P–C) _{ave}	115.3	116.1	115.7
(C–P–C) _{ave}	102.8	102.1	102.4
I–Fe–CO	90.5(6)	95.1(1)	89.4(2)
I–Fe–PPh ₃	94.2(1)	94.1(1)	97.0(0)
PPh ₃ –Fe–CO	89.2(6)	91.0(1)	91.4(2)

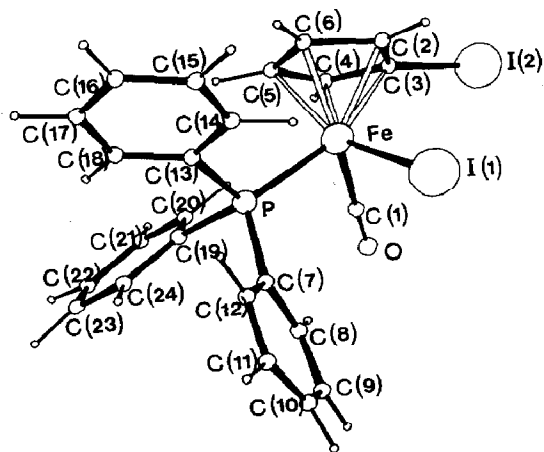
^a Cen = ring centroid.

and to establish the role of electronic and steric effects on the conformational preferences of related ring substituents.

Crystal structures. Selected bond length and bond angle data for **1** and **3** as well as a closely related complex $[(\eta^5\text{-C}_5\text{H}_4\text{tBu})\text{Fe}(\text{CO})(\text{PPh}_3)\text{I}]$ (**4**) [2] are given in Table 5. ORTEP [16] diagrams of **1** and **3** are given in Fig. 3 and 4. Figure 5 shows the projections of the molecules **1** and **3** down the Fe–Cen (Cen = centroid) axis.

The crystallographic data are insufficiently accurate to assess whether localised (allyl-ene or diene) bonding occurs in the cyclopentadienyl rings of **1** and **3**. Least squares planes calculations for the cyclopentadienyl ring and the position of the ring substituent relative to the plane were performed and are represented graphically in Fig. 6. The ring substituents are raised out the plane, away from the Fe atom by 4° and 3° for **1** and **3**, respectively.

The Fe–I bond lengths **1** (2.621(3) Å) and **3** (2.624(3) Å) are very similar to values reported for similar complexes [17–19]. The Fe–Cen distance does appear to

Fig. 3. ORTEP diagram of $[(\eta^5\text{-C}_5\text{H}_4\text{I})\text{Fe}(\text{CO})(\text{PPh}_3)\text{I}]$ (**1**).

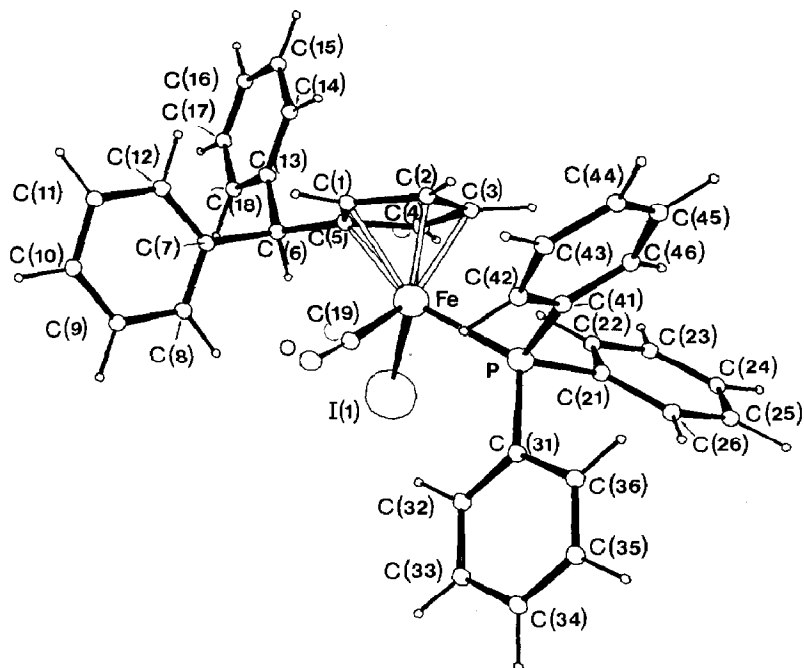


Fig. 4. ORTEP diagram of $[(\eta^5\text{-C}_5\text{H}_4\text{CHPh}_2)\text{Fe}(\text{CO})(\text{PPh}_3)\text{I}]$ (**3**).

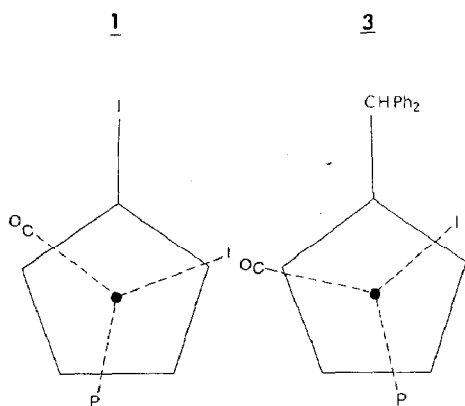


Fig. 5. Projection of **1** and **3** down the ring centroid-Fe axis.

Table 6

Selected torsion angles for **1**, **3** and **4**

Complex	Torsion ^a	Angle (°)
1	C(1)-Cen-Fe-P	-166.70
	C(1)-Cen-Fe-I	68.01
	C(1)-Cen-Fe-C(6)	-48.04
3	C(1)-Cen-Fe-P	165.54
	C(1)-Cen-Fe-I	44.12
	C(1)-Cen-Fe-C(19)	-73.0
4	C(1)-Cen-Fe-P	120.90
	C(1)-Cen-Fe-I	-116.18
	C(1)-Cen-Fe-C(10)	-1.12

^a Cen = ring centroid.

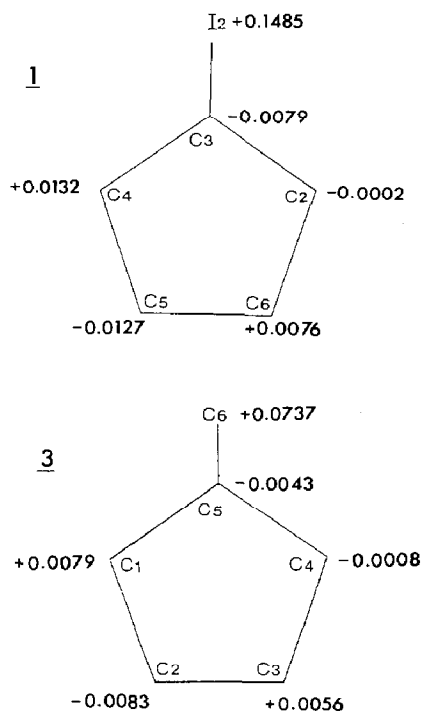


Fig. 6. Displacement of carbon and substituent atoms from the ring least squares plane for **1** and **3**.

depend on the ring substituent ($I < \text{CHPh}_2 < {}^t\text{Bu}$, Table 5), increasing with the electron-donating ability of the ring substituent. Bond angles between the Fe atom and the ligand set are again consistent with the Fe atoms' being in an octahedral environment. The local symmetry around the triphenylphosphine P atoms is near tetrahedral (Table 5).

Torsion angles quantifying the orientation of the ligand set relative to the cyclopentadienyl ring are given in Table 6. The relative dispositions of the ligand sets are qualitatively similar for **1** and **3**. Data for the related complex $[(\eta^5\text{-C}_5\text{H}_4{}^t\text{Bu})\text{Fe}(\text{CO})(\text{PPh}_3)\text{I}]$ are also listed in Table 6 for comparison.

The most significant feature of the structure of **3** relates to the conformation of the ligand set relative to the CHPh_2 substituent. The disposition of these ligands is exactly that predicted in the solution state (see above). Relative to the cyclopentadienyl plane, the benzhydryl hydrogen atom points below the plane (torsion angle C5-C1-C6-H6 49°) but towards H5. Similarly the one aryl ring lies almost perpendicular to the cyclopentadienyl ring (torsion angle C1-C6-C7-C8 98°) and points towards H2. The position of the PPh_3 lying trans to the ring substituent and close to one of the ring carbon atoms is also as observed in the ${}^1\text{H}$ NMR spectrum.

Acknowledgements

We thank the University of the Witwatersrand and the FRD for financial support.

References

- 1 P. Johnston, M.S. Loonat, W.L. Ingham, L. Carlton and N.J. Coville, *Organometallics*, 6 (1987) 2121 and ref. cited therein.
- 2 K. du Plooy, C.F. Marais, L. Carlton, R. Hunter, J.C.A. Boeyens and N.J. Coville, *Inorg. Chem.*, submitted.
- 3 J. Sandström and J. Sieta, *J. Organomet. Chem.*, 108 (1976) 371.
- 4 J. Sandström and J. Sieta, *Acta Chem. Scand. B*, 31 (1977) 86.
- 5 W. Freiesleben, *Angew. Chem. Int. Ed. Engl.*, 2 (1963) 396.
- 6 J. Thiele, *Chem. Ber.*, 33 (1900) 666; J.L. Rice and F.M. Parham, *J. Am. Chem. Soc.*, 80 (1958) 3792; D.J. Sardella, C.M. Keane, and P. Lemonias, *J. Am. Chem. Soc.*, 106 (1984) 4962.
- 7 K. Hafner, *Liebigs. Ann. Chem.*, 606 (1957) 79.
- 8 K. Ziegler, H.G. Gellert, A. Martin, K. Nagel and J. Schneider, *Liebigs. Ann. Chem.*, 589 (1954) 91.
- 9 M. Regitz and A. Liedhegener, *Tetrahedron*, 23 (1967) 2201.
- 10 T. Weil and M. Cais, *J. Org. Chem.*, 28 (1963) 2472.
- 11 W.v.E. Doering and C.H. Depuy, *J. Am. Chem. Soc.*, 75 (1953) 5955.
- 12 W.A. Herrmann and M. Huber, *Chem. Ber.*, 111 (1978) 3124.
- 13 N. Walker and D. Stuart, *Acta. Crystallog. A*, 39 (1983) 158.
- 14 SHELX-86, G.M. Sheldrick in G.M. Sheldrick, C. Krüger and R. Goddard (Eds.), *Crystallographic Computing 3*, Oxford Univ. Press, 1985.
- 15 H. Iwamura and K. Mislow, *Acc. Chem. Res.*, 21 (1988) 175 and ref. cited therein.
- 16 C.K. Johnston, ORTEP, Report ORNL-3794, 1965, Oak Ridge National Laboratory, Oak Ridge TN.
- 17 G. Balavoine, S. Brunie, H.B. Kagan, *J. Organomet.Chem.*, 187 (1980) 125.
- 18 V.D. Andrianov, Yu.A. Chapovskii, V.A. Semion and Yu.T. Struchkov, *Chem. Commun.*, (1968) 282.
- 19 T.G. Attig, R.G. Teller, S.M. Wu, R. Ban and A. Wojcicki, *J. Am. Chem. Soc.*, 101 (1979) 619.